

Rochester Institute of Technology

RIT Digital Institutional Repository

Articles

Faculty & Staff Scholarship

9-16-2008

Three-Body Equations of Motion in Successive Post-Newtonian Approximations

Carlos O. Lousto

Rochester Institute of Technology

Hiroyuki Nakano

Rochester Institute of Technology

Follow this and additional works at: <https://repository.rit.edu/article>

Recommended Citation

Carlos O Lousto and Hiroyuki Nakano 2008 Class. Quantum Grav. 25 195019

This Article is brought to you for free and open access by the RIT Libraries. For more information, please contact repository@rit.edu.

Three-body equations of motion in successive post-Newtonian approximations

Carlos O. Lousto and Hiroyuki Nakano

*Center for Computational Relativity and Gravitation, School of Mathematical Sciences,
Rochester Institute of Technology, Rochester, New York 14623, USA*

There are periodic solutions to the equal-mass three-body (and N -body) problem in Newtonian gravity. The figure-eight solution is one of them. In this paper, we discuss its solution in the first and second post-Newtonian approximations to General Relativity. To do so we derive the canonical equations of motion in the ADM gauge from the three-body Hamiltonian. We then integrate those equations numerically, showing that quantities such as the energy, linear and angular momenta are conserved down to numerical error. We also study the scaling of the initial parameters with the physical size of the triple system. In this way we can assess when general relativistic results are important and we determine that this occur for distances of the order of $100M$, with M the total mass of the system. For distances much closer than those, presumably the system would completely collapse due to gravitational radiation. This sets up a natural cut-off to Newtonian N -body simulations. The method can also be used to dynamically provide initial parameters for subsequent full nonlinear numerical simulations.

PACS numbers: 95.10.Ce, 95.30.Sf, 45.50.Pk, 04.25.Nx

I. INTRODUCTION

The closest star to the solar system, Alpha Centauri, is a triple system, so is Polaris and HD 188753. Triple stars and black holes are common in globular clusters [1, 2], and galactic disks. Triple black hole mergers can be formed in galaxy merger [3] and a triple quasar, representing a triple supermassive black hole system has been recently discovered [4].

Full numerical simulations of black holes made possible only in the last couple of years have already produced numerous astrophysically interesting results, among them, the orbital hangup and respect of the cosmic censorship hypothesis for spinning black holes [5, 6, 7], precession and spin-flips [7], and the discovery [8] of large recoil velocities in highly-spinning black hole mergers up to 4,000 km/s [9].

The 2005 breakthroughs in Numerical Relativity [10, 11, 12], not only provided a solution to the long standing two-body problem in General Relativity, but it also proved applicable to the black hole - neutron star binaries [13] and recently to the three (and N) - black holes systems [14].

In general, the solution of three-body problem in Newtonian gravity can be chaotic. There are however, periodic orbits in the problem of three equal masses on a plane. One of the most surprising solution is a figure-eight orbit. The three bodies chase each other forever around a fixed eight-shaped curve. This was found first by Moore [15] and discussed with the proof of the existence in Ref. [16]. Heggie [17] also estimates the probability for such systems to occur in a galaxy.

Because of effects such as the perihelion shift, it was unclear if the figure-eight orbits would exist in a low post-Newtonian expansion, even if it consist of only conservative terms. Imai, Chiba and Asada succeeded in obtaining the figure-eight solution in a first post-Newtonian or-

der approximation by finding the general relativistic corrections to the Newtonian initial conditions. In Ref. [18] they also estimated the periodic gravitational waves from this system.

In Ref. [19] was used the Euler-Lagrange equations of motion in an approximation to first post-Newtonian order. In our paper we instead assume the Hamiltonian formulation to derive the equations of motion. We start from the Hamiltonian given in Ref. [20] (with typos corrected in our Appendix). We derive the equations of motion in this formalism, which are different from those used in Ref. [19] and have the virtue of explicitly satisfying the constants of motion of the problem, and thus being more amenable to numerical integration.

The paper is organized as follows. In Section II, we summarize the equations of motion to be solved numerically in order to obtain the figure-eight orbits. The starting point is the three-body Hamiltonian in the first post-Newtonian approximation. In Section III, we discuss the initial conditions for the figure-eight solutions. We study the scaling relation between the orbital radius and the linear momenta. From this analysis, we can estimate when general relativistic effects are important. In Section IV, we extend our calculation to the second post-Newtonian order and in Section V, we summarize the results of this paper and discuss some remaining problems. The 2PN three-body Hamiltonian is explicitly given in the Appendix. Throughout this paper, we use units in which $c = G = 1$.

II. EQUATIONS OF MOTION

As we mentioned in the introduction, the Newtonian configuration that leads to orbital braid figures can also be obtained within the Lagrangian approach, in the first post-Newtonian approximation, by finding the appropri-

ate corrections to the initial data [19].

Here we will consider the Hamiltonian formulation since it generates equations of motion that conserve the energy, linear and angular momenta. This is crucial to reach high accuracy in the numerical integrations, which is needed to keep good track of the orbital motion, that in the three body problem might be chaotic.

The Hamiltonian ($H = H_N + H_{1PN} + H_{2PN}$) for the three body problem in the second post-Newtonian approximation is given next. Note that since gravitational radiation only enters at 2.5PN-order and higher, the current analysis applies to conservative systems.

The Newtonian Hamiltonian is given by

$$H_N = \frac{1}{2} \sum_a \frac{p_a^2}{m_a} - \frac{1}{2} \sum_{a,b \neq a} \frac{m_a m_b}{r_{ab}}, \quad (1)$$

and to the first post-Newtonian order by

$$\begin{aligned} H_{1PN} = & -\frac{1}{8} \sum_a m_a \left(\frac{p_a^2}{m_a^2} \right)^2 \\ & -\frac{1}{4} \sum_{a,b \neq a} \frac{m_a m_b}{r_{ab}} \left\{ 6 \frac{p_a^2}{m_a^2} - 7 \frac{\mathbf{p}_a \cdot \mathbf{p}_b}{m_a m_b} \right. \\ & \left. - \frac{(\mathbf{n}_{ab} \cdot \mathbf{p}_a)(\mathbf{n}_{ab} \cdot \mathbf{p}_b)}{m_a m_b} \right\} \\ & + \frac{1}{2} \sum_{a,b \neq a, c \neq a} \frac{m_a m_b m_c}{r_{ab} r_{ac}}, \end{aligned} \quad (2)$$

where a, b and c run over 1, 2 and 3. We have used the notations; $\mathbf{x}_{ab} = \mathbf{x}_a - \mathbf{x}_b$, $r_{ab} = |\mathbf{x}_{ab}|$, $\mathbf{n}_{ab} = \mathbf{x}_{ab}/r_{ab}$, $p_a^2 = \mathbf{p}_a \cdot \mathbf{p}_a$ and the dot (\cdot) means the inner product. The Hamiltonian for the second post-Newtonian order is given in the Appendix.

We then obtain the canonical equations

$$(\dot{p}_a)_i = -\frac{\partial H}{\partial (q_a)_i}, \quad (\dot{q}_a)_i = \frac{\partial H}{\partial (p_a)_i}, \quad (3)$$

where i denotes x, y or z .

Explicitly, the equation of motion for the first post-Newtonian order, are given for the particle 1 by

$$\begin{aligned} \frac{\partial}{\partial t} \mathbf{x}_1 = & \frac{\mathbf{p}_1}{m_1} - \frac{1}{2} \frac{(\mathbf{p}_1 \cdot \mathbf{p}_1) \mathbf{p}_1}{m_1^3} \\ & - \frac{1}{2} \frac{m_1 m_2}{r_{12}} \left(\frac{6 \mathbf{p}_1}{m_1^2} - \frac{7}{m_1 m_2} \frac{\mathbf{p}_2}{r_{12}} \right. \\ & \left. - \frac{(\mathbf{p}_2 \cdot \mathbf{x}_{12}) \mathbf{x}_{12}}{m_1 m_2 r_{12}^2} \right) \\ & + \frac{1}{2} \left(\frac{7}{2} \frac{\mathbf{p}_3}{r_{31}} + \frac{1}{2} \frac{(\mathbf{p}_3 \cdot \mathbf{x}_{31}) \mathbf{x}_{31}}{r_{31}^3} \right) \\ & - \frac{1}{2} \frac{m_1 m_3}{r_{31}} \left(\frac{6 \mathbf{p}_1}{m_1^2} - \frac{7}{m_1 m_3} \frac{\mathbf{p}_3}{r_{31}} \right. \\ & \left. - \frac{(\mathbf{p}_3 \cdot \mathbf{x}_{31}) \mathbf{x}_{31}}{m_3 m_1 r_{31}^2} \right) \end{aligned}$$

$$+ \frac{1}{2} \left(\frac{7}{2} \frac{\mathbf{p}_2}{r_{12}} + \frac{1}{2} \frac{(\mathbf{p}_2 \cdot \mathbf{x}_{12}) \mathbf{x}_{12}}{r_{12}^3} \right), \quad (4)$$

$$\begin{aligned} \frac{\partial}{\partial t} \mathbf{p}_1 = & -\frac{\mathbf{x}_{12}}{r_{12}} \left(\frac{m_1 m_2}{r_{12}^2} - \frac{m_2 m_1 m_3}{r_{12}^2 r_{2,3}} - \frac{m_1 m_2 m_3}{r_{12}^2 r_{31}} \right. \\ & + \frac{1}{2} \frac{m_1 m_2}{r_{12}^2} \left(\frac{3(\mathbf{p}_1 \cdot \mathbf{p}_1)}{m_1^2} + \frac{3(\mathbf{p}_2 \cdot \mathbf{p}_2)}{m_2^2} \right. \\ & \left. - \frac{7(\mathbf{p}_1 \cdot \mathbf{p}_2)}{m_1 m_2} - \frac{(\mathbf{p}_1 \cdot \mathbf{x}_{12})(\mathbf{p}_2 \cdot \mathbf{x}_{12})}{m_1 m_2 r_{12}^2} \right) \\ & \left. - \frac{(\mathbf{p}_1 \cdot \mathbf{x}_{12})(\mathbf{p}_2 \cdot \mathbf{x}_{12})}{r_{12}^4} - \frac{m_2 m_1^2}{r_{12}^3} - \frac{m_1 m_2^2}{r_{12}^3} \right) \\ & + \frac{\mathbf{x}_{31}}{r_{31}} \left(\frac{m_3 m_1}{r_{31}^2} - \frac{m_3 m_1 m_2}{r_{31}^2 r_{2,3}} - \frac{m_1 m_2 m_3}{r_{12} r_{31}^2} \right. \\ & + \frac{1}{2} \frac{m_3 m_1}{r_{31}^2} \left(\frac{3(\mathbf{p}_3 \cdot \mathbf{p}_3)}{m_3^2} + \frac{3(\mathbf{p}_1 \cdot \mathbf{p}_1)}{m_1^2} \right. \\ & \left. - \frac{7(\mathbf{p}_1 \cdot \mathbf{p}_3)}{m_1 m_3} - \frac{(\mathbf{p}_3 \cdot \mathbf{x}_{31})(\mathbf{p}_1 \cdot \mathbf{x}_{31})}{m_3 m_1 r_{31}^2} \right) \\ & \left. - \frac{(\mathbf{p}_3 \cdot \mathbf{x}_{31})(\mathbf{p}_1 \cdot \mathbf{x}_{31})}{r_{31}^4} - \frac{m_3 m_1^2}{r_{31}^3} - \frac{m_1 m_3^2}{r_{31}^3} \right) \\ & - \frac{1}{2} \left(\frac{(\mathbf{p}_2 \cdot \mathbf{x}_{12}) \mathbf{p}_1}{r_{12}^3} + \frac{(\mathbf{p}_1 \cdot \mathbf{x}_{12}) \mathbf{p}_2}{r_{12}^3} \right) \\ & + \frac{1}{2} \left(\frac{(\mathbf{p}_1 \cdot \mathbf{x}_{31}) \mathbf{p}_3}{r_{31}^3} + \frac{(\mathbf{p}_3 \cdot \mathbf{x}_{31}) \mathbf{p}_1}{r_{31}^3} \right), \end{aligned} \quad (5)$$

where to obtain the equation of motion for the particle 2 (and 3), we change the subscripts as $\{1 \rightarrow 2, 2 \rightarrow 3, 3 \rightarrow 1\}$ (and $\{1 \rightarrow 3, 2 \rightarrow 1, 3 \rightarrow 2\}$), respectively.

We solved the above equations numerically for three body problems using a 10 digits precision implemented in *Maple* 10 with typical runs of a few seconds on a Laptop. Since we use the canonical momentum in the calculation, the Hamiltonian H , the total linear momentum $\mathbf{P} = \sum \mathbf{p}_a$ and angular momentum $\mathbf{L} = \sum \mathbf{x}_a \times \mathbf{p}_a$ are conserved quantities. These represent useful checks of the accuracy of the numerical runs.

III. THE FIRST POST-NEWTONIAN CORRECTIONS

In the Newtonian case, a figure-eight motion can be obtained from the following initial conditions [19], i.e., the positions \mathbf{l} and linear momenta \mathbf{p} :

$$\begin{aligned} \mathbf{l} &= (x_1, y_1) = (-x_2, -y_2) \\ &= (97.00, -24.31), \\ (x_3, y_3) &= (0, 0), \\ \mathbf{p}_N &= (p_3^x, p_3^y) = (-2p_1^x, -2p_1^y) = (-2p_2^x, -2p_2^y) \\ &= (-0.09324, -0.08647). \end{aligned} \quad (6)$$

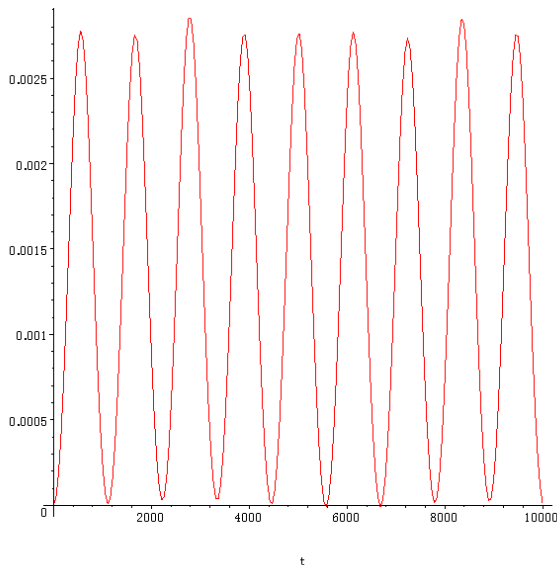


FIG. 1: The relative error of the Hamiltonian constraint in the Lagrangian approximation. This figure is derived by using the orbit in [19].

Here, we set $m_1 = m_2 = m_3 = m = 1$. For the above initial condition, the total linear momentum and angular momentum are zero.

At the 1PN order, we also impose the total linear momentum $\mathbf{P} = 0$ and the total angular momentum $\mathbf{L} = 0$. By these conditions, we find that each linear momentum is given by the relations

$$\mathbf{p}_3 = -2\mathbf{p}_1 = -2\mathbf{p}_2. \quad (7)$$

Therefore, when we give the positions of the three particles, and it is necessary then only to search numerically for \mathbf{p}_3 . In order to obtain, \mathbf{p}_3 , we make some iterative computations until the figure-eight is reproduced for a few orbits.

In Figures 1 and 2 we show the relative error of the Hamiltonian conservation:

$$\Delta H(t) = \frac{H(t) - H(0)}{H(0)}.$$

Figure 1 is estimated by using the orbit calculated in [19] and we observe that they lead to violations of the order of 3×10^{-3} . While, Figure 2 is derived by using the canonical equations derived in our paper and they display errors of the order of 10^{-6} , growing linearly in time due to the propagation of numerical errors triggered by initial roundoff.

Next we will discuss the scaling behavior of \mathbf{p}_3 when we change the initial separation as $\mathbf{l} \rightarrow \lambda \mathbf{l}$, and hence the size of the orbit. Note that $\mathbf{p}_3 \rightarrow \lambda^{-1/2} \mathbf{p}_3$ in the Newtonian limit as can be easily derived from the Hamiltonian in Eq. (1) or the equations of motion (4).

In Table I, we summarize our numerical findings for the 1PN initial conditions for λ from 1 to 100. We note

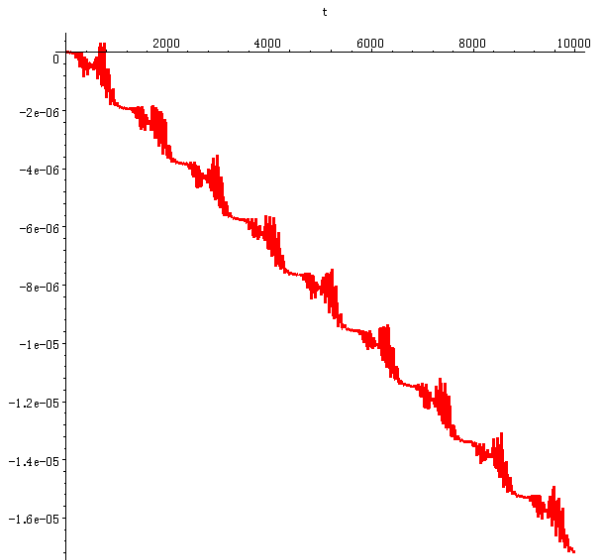


FIG. 2: The relative error of the Hamiltonian constraint evaluate by using the orbit derived from the Hamiltonian formalism.

TABLE I: The initial conditions and inclination angle.

λ	$(p_3)_x$	$(p_3)_y$	θ
1.00	-0.09811067089	-0.09490870640	0.01535863098
2.00	-0.06754964265	-0.06392246619	0.007238984240
5.00	-0.04209168100	-0.03934705365	0.002786451510
10.00	-0.02961805051	-0.02758150399	0.001351084509
20.00	-0.02089989478	-0.01941808121	0.0006871250545
50.00	-0.01319661317	-0.01225031026	0.0002447024114
100.00	-0.009328662000	-0.008654573162	0.0001269692928

that \mathbf{p}_3 with $\lambda = 1$ is different from the value which are derived from the initial velocity of [19]. The value θ in the table is the inclination angle of the principal axes. The principal axes of the 1PN figure-eight motion are not along the x and y axes [19].

In Figure 3, the figure-eight rescaled orbits with $\lambda = 1, 10$ and 100 are shown. Here, in order to display the general relativistic effects, we have used the coordinates: $(x_a(t)/\lambda, y_a(t)/\lambda)$. We have chosen here the x-axis as the principal axis. We observe that the superposition of the $\lambda = 10$ and $\lambda = 100$ is suggestive that at those scales the general relativistic effects are very small while for $\lambda < 1$ they are dominant, but remainder gauge effects may also mask this effect because the orbits are not gauge invariant. A cleaner analysis can be made directly looking at the initial linear momenta scaling.

By using the results of the runs in Table I, we propose a fitting formula for $|\mathbf{p}_3|$ inspired again in the 1PN

$$|\mathbf{p}_3|_{\text{fit}}(\lambda) = \sqrt{\frac{0.01617387234}{\lambda} + \frac{0.002042558971}{\lambda^2} + \frac{0.0004169461512}{\lambda^3}}. \quad (8)$$

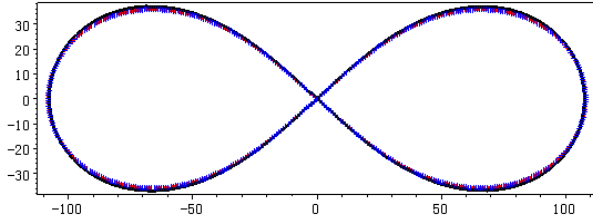


FIG. 3: Figure-eight motions. We show $\lambda = 1$ (solid line) $\lambda = 10$ (dashed line) and $\lambda = 100$ (dotted line).

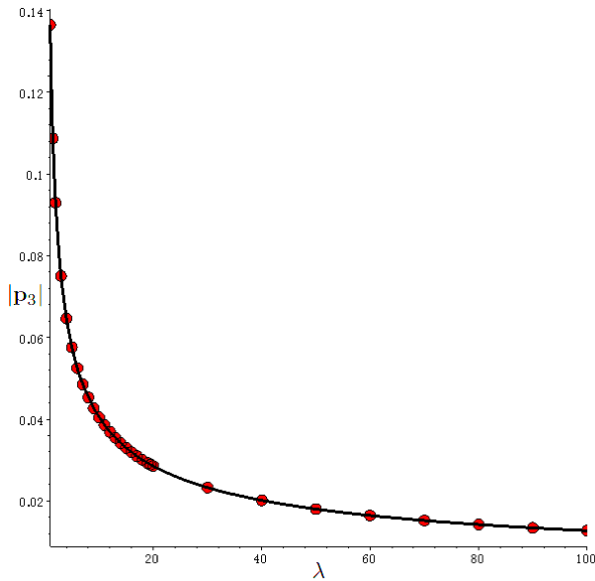


FIG. 4: λ - $|\mathbf{p}_3|$ relation with points obtained numerically.

In Figure 4, we show the fitting function and in Figure 5 we display the relative error $|\mathbf{p}_3| - |\mathbf{p}_3|_{\text{fit}}/|\mathbf{p}_3|$, consistent with the form of an error generated in the numerical calculation.

Independently in the Newtonian calculations, the λ - $|\mathbf{p}_3|$ relation can be obtained from the initial condition in Eqs. (6) as

$$|\mathbf{p}_3|_N(\lambda) = \frac{0.1271642973}{\lambda^{1/2}}. \quad (9)$$

Note that relative difference $|\mathbf{p}_3|$ between the Newtonian

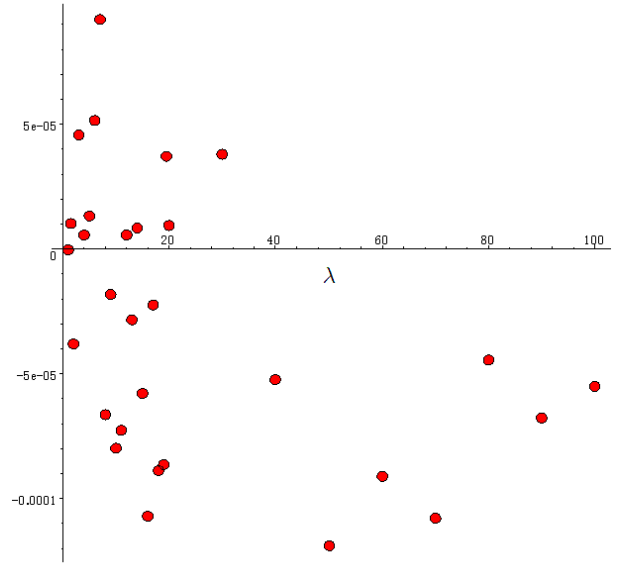


FIG. 5: The relative error of the fitting.

and the first post-Newtonian calculations:

$$\frac{|\mathbf{p}_3|_{\text{fit}}(\lambda) - |\mathbf{p}_3|_N(\lambda)}{|\mathbf{p}_3|_N(\lambda)},$$

is 7% for $\lambda = 1$, 0.6% for $\lambda = 10$ and 0.07% for $\lambda = 100$.

IV. SECOND POST-NEWTONIAN CORRECTIONS

It is interesting to verify if this kind of orbits also exists in the second post-Newtonian approximation to General Relativity, since they incorporate further effects of the curvature, but yet not gravitational radiation. The calculations are done by using the same method as for the first post-Newtonian order. In Table II, we summarize the initial conditions for each λ from 1 to 100. We show the numerical errors as measured through the Hamiltonian non-conservation in Figure 6.

We find that we can approximate $|\mathbf{p}_3|$ by the fitting formula

$$|\mathbf{p}_3|_{\text{fit}}(\lambda) = \sqrt{\frac{0.01617654493}{\lambda} + \frac{0.002017242451}{\lambda^2} + \frac{0.0002017242451}{\lambda^3} + \frac{0.0001054698539}{\lambda^4}}. \quad (10)$$

TABLE II: The initial conditions and inclination angle for the second post-Newtonian case.

λ	$(p_3)_x$	$(p_3)_y$	θ
1.00	-0.09759146109	-0.09386471063	0.01335212441
2.00	-0.06746813797	-0.06375625776	0.006775950067
5.00	-0.04208326266	-0.03933131483	0.002713363325
10.00	-0.02961805051	-0.02757874584	0.001340868765
20.00	-0.02089780479	-0.01941808121	0.0006733410290
50.00	-0.01319661317	-0.01225031026	0.0002447024114
100.00	-0.009328662000	-0.008654573162	0.0001269692928

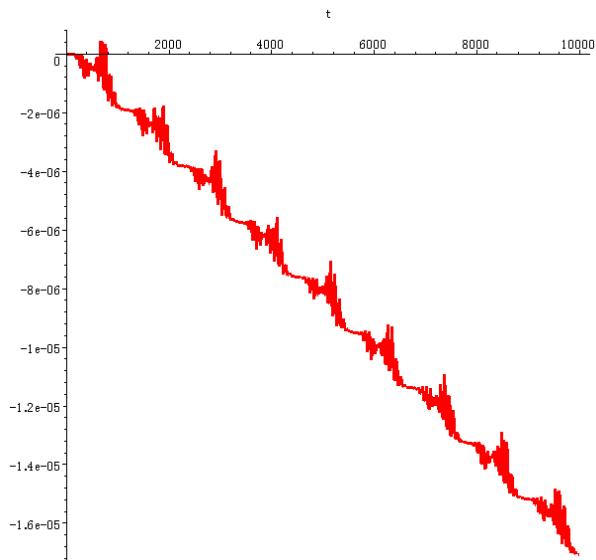


FIG. 6: The relative error of the Hamiltonian conservation for the second post-Newtonian order calculations.

There is a significant difference between the coefficient of $1/\lambda^3$ in Eqs. (8) and (10). This is due to second post-Newtonian corrections entering in this coefficient, as we can verify from the form of the Hamiltonian.

In Figure 7, we show the fitting function while its relative error is given in Figure 8.

Finally, we summarize the results by showing the difference between the Newtonian, first and second post-Newtonian results in Figure 9. The second post-Newtonian effect is small but clearly not negligible for $\lambda = 1$.

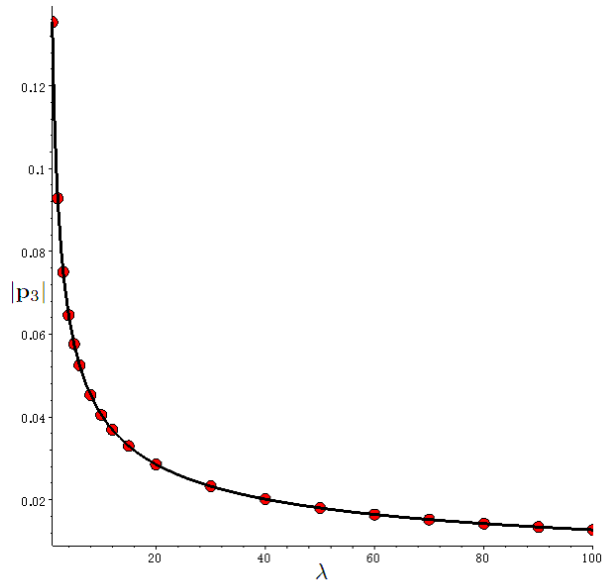


FIG. 7: λ - $|\mathbf{p}_3|$ relation for the second post-Newtonian case. The points are obtained numerically.

V. DISCUSSION

In this paper we have used the figure-eight orbits as a theoretical lab to test the properties of the low post-Newtonian expansions of General Relativity. We have found that those closed orbits exist for three (and presumably N) bodies. We have provided an improved first-post-Newtonian order formalism for deriving the equations of motion that satisfy the Hamiltonian (the linear and angular momenta) constraint to round-off error. The subsequent numerical evolution is well behaved during for more than $t \sim 10,000m$. We have also extended this analysis to the $2PN$ corrections, still giving a conservative system of equations. In the process of finding the figure-eight solutions by trial of different initial momenta we also showed (numerically) the stability of the orbit against small perturbations.

This method is particularly useful to determine, dynamically (as an alternative to determine them through families of initial data [21]), initial orbital parameters for subsequent full numerical evolution [14], when the holes are close enough that general relativistic effects can no longer be ignored. Note that our method fully takes into account the three-body post-Newtonian interactions unlike other simulations that approximate the problem in successive two-body problems [22].

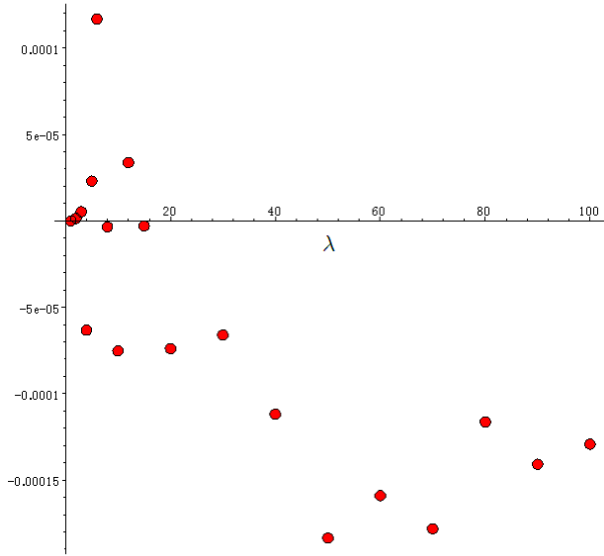


FIG. 8: The relative fitting error for the second post-Newtonian case.

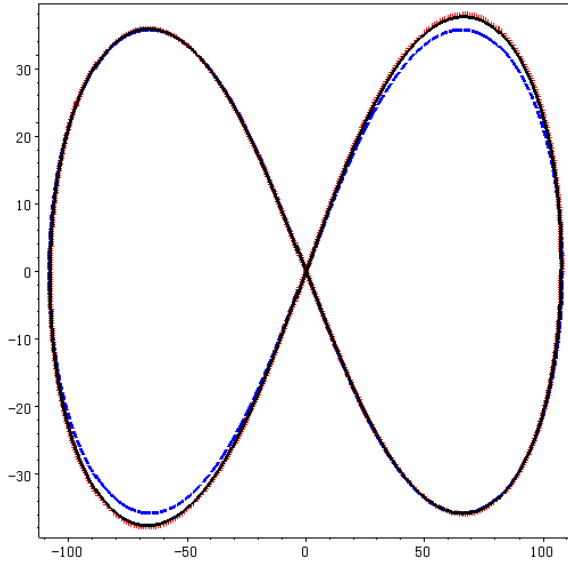


FIG. 9: Comparison of figure-eight motions for $\lambda = 1$. The solid, dotted and dashed lines show the 2PN, 1PN and Newtonian results, respectively.

It is interesting to note here that the scaling fits (10) give a practical way to determine when relativistic or Newtonian approaches are appropriate. For $\lambda = 1$ we have that the ratio of the first coefficient, 0.01617654493 (Newtonian) to the second coefficient 0.002017242451 (first-post-Newtonian) is nearly $0.12/\lambda$ and the second coefficient to the third one 0.0002463605227 (dominated by second-post-Newtonian) is also approximately $0.12/\lambda$. This indicates that post-Newtonian corrections are important. For $\lambda = 1$ the distance between the initial bodies is $200m$, what indicates that for nearly $67M$ with $M \approx 3m$ the total mass of the system has strong post-Newtonian effects. For $\lambda \gg 1$ Newtonian gravity should describe the system accurately, while for $\lambda < 1$ general relativistic effects should be very important, eventually leading to the total collapse of the system. It is interesting to remark here that most of the N -body codes use some sort of regularization of the Newtonian gravity for very close encounters [23], instead the natural way to regularize these close encounters [14] is given by the General Theory of Relativity, and as we show here, the post-Newtonian corrections are already non-negligible at separations of the order of $100M$. In any case, for most of the astrophysical encounters this is way too short distance, but it can obviously be reached in systems involving black holes and neutron stars.

Acknowledgments

We would like to thank H.-P. Bischof, M. Campanelli, A. Gualandris, D. Merritt, D. Ross and Y. Zlochower for useful discussions. This is supported by JSPS for Research Abroad (HN) and by the NSF through grants PHY-0722315, PHY-0701566, PHY-0714388, and PHY-0722703.

APPENDIX A: THE SECOND POST-NEWTONIAN THREE-BODY HAMILTONIAN

In this appendix, we give explicitly the Hamiltonian for the three body problem at second post-Newtonian order in the ADM gauge since there are some typos in the summation of [20]. The equations of motion used in our paper can be derived straightforwardly from this Hamiltonian, but are too cumbersome to write down here.

$$\begin{aligned}
 H_{2PN} = & \frac{1}{16} \sum_a m_a \left(\frac{p_a^2}{m_a^2} \right)^3 + \frac{1}{16} \sum_{a,b \neq a} \frac{m_a m_b}{r_{ab}} \left\{ 10 \left(\frac{p_a^2}{m_a^2} \right)^2 - 11 \frac{p_a^2 p_b^2}{m_a^2 m_b^2} - 2 \frac{(\mathbf{p}_a \cdot \mathbf{p}_a)^2}{m_a^2 m_b^2} \right. \\
 & \left. + 10 \frac{p_a^2 (\mathbf{n}_{ab} \cdot \mathbf{p}_b)^2}{m_a^2 m_b^2} - 12 \frac{(\mathbf{p}_a \cdot \mathbf{p}_b) (\mathbf{n}_{ab} \cdot \mathbf{p}_a) (\mathbf{n}_{ab} \cdot \mathbf{p}_b)}{m_a^2 m_b^2} - 3 \frac{(\mathbf{n}_{ab} \cdot \mathbf{p}_a)^2 (\mathbf{n}_{ab} \cdot \mathbf{p}_b)^2}{m_a^2 m_b^2} \right\}
 \end{aligned}$$

$$\begin{aligned}
& + \frac{1}{8} \sum_{a,b \neq a, c \neq a} \frac{m_a m_b m_c}{r_{ab} r_{ac}} \left\{ 18 \frac{p_a^2}{m_a^2} + 14 \frac{p_b^2}{m_b^2} - 2 \frac{(\mathbf{n}_{ab} \cdot \mathbf{p}_b)^2}{m_b^2} - 50 \frac{\mathbf{p}_a \cdot \mathbf{p}_b}{m_a m_b} + 17 \frac{\mathbf{p}_b \cdot \mathbf{p}_c}{m_b m_c} \right. \\
& - 14 \frac{(\mathbf{n}_{ab} \cdot \mathbf{p}_a)(\mathbf{n}_{ab} \cdot \mathbf{p}_b)}{m_a m_b} + 14 \frac{(\mathbf{n}_{ab} \cdot \mathbf{p}_b)(\mathbf{n}_{ab} \cdot \mathbf{p}_c)}{m_b m_c} + \mathbf{n}_{ab} \cdot \mathbf{n}_{ac} \frac{(\mathbf{n}_{ab} \cdot \mathbf{p}_b)(\mathbf{n}_{ac} \cdot \mathbf{p}_c)}{m_b m_c} \left. \right\} \\
& + \frac{1}{8} \sum_{a,b \neq a, c \neq a} \frac{m_a m_b m_c}{r_{ab}^2} \left\{ 2 \frac{(\mathbf{n}_{ab} \cdot \mathbf{p}_a)(\mathbf{n}_{ac} \cdot \mathbf{p}_c)}{m_a m_c} + 2 \frac{(\mathbf{n}_{ab} \cdot \mathbf{p}_b)(\mathbf{n}_{ac} \cdot \mathbf{p}_c)}{m_a m_c} \right. \\
& + 5 \mathbf{n}_{ab} \cdot \mathbf{n}_{ac} \frac{p_c^2}{m_c^2} - \mathbf{n}_{ab} \cdot \mathbf{n}_{ac} \frac{(\mathbf{n}_{ac} \cdot \mathbf{p}_c)^2}{m_c^2} - 14 \frac{(\mathbf{n}_{ab} \cdot \mathbf{p}_c)(\mathbf{n}_{ac} \cdot \mathbf{p}_c)}{m_c^2} \left. \right\} \\
& + \frac{1}{4} \sum_{a,b \neq a} \frac{m_a^2 m_b}{r_{ab}^2} \left\{ \frac{p_a^2}{m_a^2} + \frac{p_b^2}{m_b^2} - 2 \frac{\mathbf{p}_a \cdot \mathbf{p}_b}{m_a m_b} \right\} \\
& + \frac{1}{2} \sum_{a,b \neq a, c \neq a, b} \frac{m_a m_b m_c}{(r_{ab} + r_{bc} + r_{ca})^2} (n_{ab}^i + n_{ac}^i)(n_{ab}^j + n_{cb}^j) \left\{ 8 \frac{p_{ai} p_{cj}}{m_a m_c} - 16 \frac{p_{aj} p_{ci}}{m_a m_c} \right. \\
& + 3 \frac{p_{ai} p_{bj}}{m_a m_b} + 4 \frac{p_{ci} p_{cj}}{m_c^2} + \frac{p_{ai} p_{aj}}{m_a^2} \left. \right\} \\
& + \frac{1}{2} \sum_{a,b \neq a, c \neq a, b} \frac{m_a m_b m_c}{(r_{ab} + r_{bc} + r_{ca}) r_{ab}} \left\{ 8 \frac{\mathbf{p}_a \cdot \mathbf{p}_c - (\mathbf{n}_{ab} \cdot \mathbf{p}_a)(\mathbf{n}_{ab} \cdot \mathbf{p}_c)}{m_a m_c} \right. \\
& - 3 \frac{\mathbf{p}_a \cdot \mathbf{p}_b - (\mathbf{n}_{ab} \cdot \mathbf{p}_a)(\mathbf{n}_{ab} \cdot \mathbf{p}_b)}{m_a m_b} - 4 \frac{p_c^2 - (\mathbf{n}_{ab} \cdot \mathbf{p}_c)^2}{m_c^2} - \frac{p_a^2 - (\mathbf{n}_{ab} \cdot \mathbf{p}_a)^2}{m_a^2} \left. \right\} \\
& - \frac{1}{2} \sum_{a,b \neq a, c \neq b} \frac{m_a^2 m_b m_c}{r_{ab}^2 r_{bc}} - \frac{1}{4} \sum_{a,b \neq a, c \neq a} \frac{m_a m_b m_c^2}{r_{ab} r_{ac}^2} + \frac{1}{2} \sum_{a,b \neq a} \frac{m_a^3 m_b}{r_{ab}^3} \\
& - \frac{3}{4} \sum_{a,b \neq a, c \neq a} \frac{m_a^2 m_b m_c}{r_{ab}^2 r_{ac}} - \frac{3}{8} \sum_{a,b \neq a, c \neq a, b} \frac{m_a^2 m_b m_c}{r_{ab} r_{ac} r_{bc}} + \frac{3}{8} \sum_{a,b \neq a} \frac{m_a^2 m_b^2}{r_{ab}^3} \\
& - \frac{1}{64} \sum_{a,b \neq a, c \neq a, b} \frac{m_a^2 m_b m_c}{r_{ab}^3 r_{ac}^3 r_{bc}} \{ 18 r_{ab}^2 r_{ac}^2 - 60 r_{ab}^2 r_{bc}^2 - 24 r_{ab}^2 r_{ac} (r_{ab} + r_{bc}) + 60 r_{ab} r_{ac} r_{bc}^2 + 56 r_{ab}^3 r_{bc} \\
& - 72 r_{ab} r_{bc}^3 + 35 r_{bc}^4 + 6 r_{ab}^4 \} - \frac{1}{4} \sum_{a,b \neq a} \frac{m_a^2 m_b^2}{r_{ab}^3}. \tag{A1}
\end{aligned}$$

-
- | | |
|---|--|
| <p>[1] K. Gultekin, M. C. Miller, and D. P. Hamilton, AIP Conf. Proc. 686, 135 (2003), astro-ph/0306204.</p> <p>[2] M. C. Miller and D. P. Hamilton (2002), astro-ph/0202298.</p> <p>[3] M. J. Valtonen, MNRAS 278, 186 (1996).</p> <p>[4] S. G. Djorgovski et al. (2007), astro-ph/0701155.</p> <p>[5] M. Campanelli, C. O. Lousto, and Y. Zlochower, Phys. Rev. D 74, 041501(R) (2006), gr-qc/0604012.</p> <p>[6] M. Campanelli, C. O. Lousto, and Y. Zlochower, Phys. Rev. D 74, 084023 (2006), astro-ph/0608275.</p> <p>[7] M. Campanelli, C. O. Lousto, Y. Zlochower, B. Krishnan, and D. Merritt, Phys. Rev. D 75, 064030 (2007), gr-qc/0612076.</p> <p>[8] M. Campanelli, C. O. Lousto, Y. Zlochower, and D. Merritt, Astrophys. J. 659, L5 (2007), gr-qc/0701164.</p> <p>[9] M. Campanelli, C. O. Lousto, Y. Zlochower, and D. Merritt, Phys. Rev. Lett. 98, 231102 (2007), gr-qc/0702133.</p> <p>[10] F. Pretorius, Phys. Rev. Lett. 95, 121101 (2005), gr-qc/0507014.</p> | <p>[11] M. Campanelli, C. O. Lousto, P. Marronetti, and Y. Zlochower, Phys. Rev. Lett. 96, 111101 (2006), gr-qc/0511048.</p> <p>[12] J. G. Baker, J. Centrella, D.-I. Choi, M. Koppitz, and J. van Meter, Phys. Rev. Lett. 96, 111102 (2006), gr-qc/0511103.</p> <p>[13] J. A. Faber, T. W. Baumgarte, Z. B. Etienne, S. L. Shapiro, and K. Taniguchi (2007), arXiv:0708.2436 [gr-qc].</p> <p>[14] M. Campanelli, C. O. Lousto, and Y. Zlochower (2007), arXiv:0710.0879 [gr-qc].</p> <p>[15] C. Moore, Physical Review Letters 70, 3675 (1993).</p> <p>[16] A. Chenciner and R. Montgomery, Ann. Math. 152, 881 (2000).</p> <p>[17] D. C. Heggie, Mon. Not. R. Astr. Soc. 318, L61 (2000), arXiv:astro-ph/9604016.</p> <p>[18] T. Chiba, T. Imai, and H. Asada, Mon. Not. Roy. Astron. Soc. 377, 269 (2007), astro-ph/0609773.</p> <p>[19] T. Imai, T. Chiba, and H. Asada, Phys. Rev. Lett. 98,</p> |
|---|--|

- 201102 (2007), gr-qc/0702076.
- [20] G. Schäfer, Phys. Lett. A **123**, 336 (1987).
- [21] M. Campanelli, M. Dettwyler, M. Hannam, and C. O. Lousto, Phys. Rev. **D74**, 087503 (2006), astro-ph/0509814.
- [22] S. J. Aarseth, Mon. Not. Roy. Astron. Soc. **378**, 285 (2007), astro-ph/0701612.
- [23] S. J. Aarseth, *Gravitational N-Body Simulations* (Gravitational N-Body Simulations, by Sverre J. Aarseth, pp. 430. ISBN 0521432723. Cambridge, UK: Cambridge University Press, November 2003., 2003).